RESEARCH PAPERS
FACULTY OF MATERIALS SCIENCE AND TECHNOLOGY IN TRNAVA
SLOVAK UNIVERSITY OF TECHNOLOGY IN BRATISLAVA

2019 Volume 27, Number 45

DESIGN OF THE MACHINE PARTS SUBJECTED TO ELASTIC-PLASTIC CONTACT CONDITIONS

Michal KRÁČALÍK

UNTERE HAUPTSTRAßE 48/5, 2424 ZURNDORF, AUSTRIA
e-mail: michal.kracalik@gmail.com
Received 27 August 2019, accepted 26 September 2019, published 29 November 2019

Abstract

The paper deals with a methodology of designing the machine parts subjected to elastic-plastic contact conditions. Elastic-plastic contact conditions are simulated by finite element (FE) simulation. As the result, the estimation of contact loading stresses in practice can be made using contact geometry, material datasheet or tensile test.

Key words

Contact, finite element, plastic deformation

INTRODUCTION

Contact loading appears in many engineering applications such as tools [1], screws [2], gears [3], crossing [4], shot peening and fretting [5] or a wheel/rail and twin-disc [6].

The machine parts are usually designed in such way that plastic deformation cannot theoretically occur. However, owing to loading conditions, plastic deformation often plays role in the lifecycle of the loaded part [6, 7]. Therefore, proper estimation of the contact loading stresses is crucial. The contact loading stresses can be obtained either experimentally [8, 9, 10, 11] which is a relatively complicated process, or numerically [12, 13, 14], but the implication on the designing the machine part according to the author are absent. Therefore, after numerical analysis, a methodology of the designing the machine parts subjected to elastic-plastic contact conditions is suggested.

FE AND MATERIAL MODEL

FE symmetric model consists of a bottom fixed part ("Cylinder") and an upper moving part ("Indenter"), see Figure 1. Performed is the static structural analysis with nominally flat contact surfaces in ANSYS 16.

Force is applied through the remote point to the upper part of the indenter. The cylinder is fixed at the bottom part. The cyclic symmetry region is chosen to revolve the model around Y-axis. Mesh size is refined up to 0.1 mm in the contact zone. Diameter of the cylinder and

indenter is 16 mm. Height of the cylinder is 20 mm. Total number of DOF is 17888. The penalty contact method is used in the FE model.

The bottom part is made of a steel material 1.4545, and the upper part of an indenter material. Chemical composition of a 1.4545 material is listed in Table 1. The bilinear material model of 1.4545 is used in the paper. Indenter material is modelled according to elastic-linear material model, using Young´s modulus E=620 GPa and Poisson ratio ν=0.3.

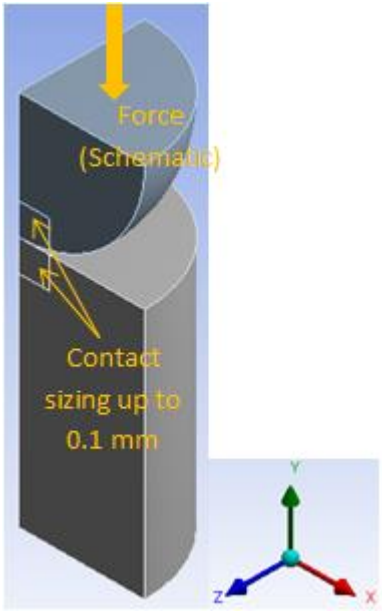

Figure 1 *Model with coordinate system*

Table 1 Chemical composition of 1.4545 [15]

C [%]	Si [≤%]	Mn [≤%]	P [≤%]	S [≤%]	Cr [%]	Mo [%]	Ni [%]	Cu [%]	Nb [%]
≤0.07	1.00	1.00	0.03	0.015	15.0-15.5	0.50	3.00-5.50	2.50-4.50	≥5xC

The bilinear material model is built via the estimation of the strain $\varepsilon_{pl_{R_m}}$ at the tensile strength R_m [MPa]. According to [15], elongation is A_5≥10%, and in [16] elongation is 16%. The estimated $\varepsilon_{pl_{R_m}}$ is 13.5% and the resulting tangent modulus T [MPa] is calculated as:

$$T = \frac{R_m - R_{p0,2}}{\varepsilon_{pl_{R_m}} - \frac{R_{p0,2}}{E}}, \tag{1}$$

where $R_{p0,2}$ is yield strength [MPa].

The calculated stress-strain curve with added elastic strain ε_{el} is shown in Figure 2. ε_{el} is true elastic strain and is plotted by creating a line connecting 0 true strain and true strain at $R_{p0,2}$. True strain is calculated as:

$$\varepsilon = \varepsilon_{el} + \varepsilon_{pl} \, . \tag{2}$$

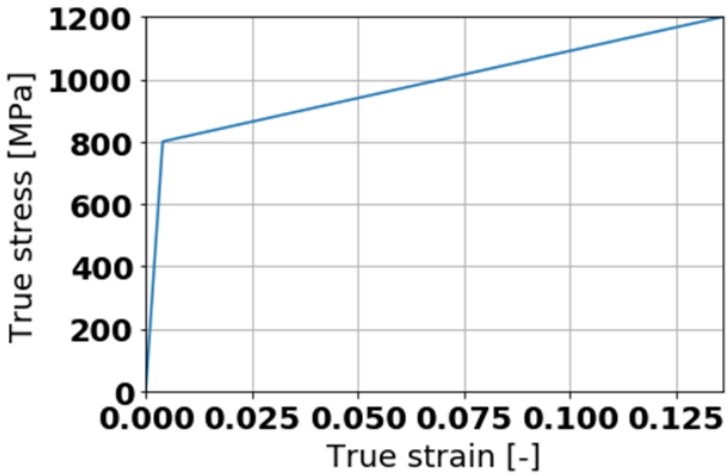

Figure 2 *True stress-strain curve of steel 1.4545 calculated by Equations (1-2)*

Table 2 Mechanical properties of 1.4545 [15, 16] and parameters of material model used in ANSYS						
$R_{p0,2}$ [MPa]	R_m [MPa]	A_5 [%]	E [GPa]	ρ [kg/m^3]	ν [-]	T [MPa]
800	1200	16	200	7800	0.3	3029.48

RESULTS

Contact pressure (Force=200 N) on the cylinder is shown in Figure 3. Figure 4 shows comparison of the computed contact pressure with Hertz (linear-elastic) contact pressure; the equations for calculating the Hertz contact pressure can be found for instance in [17].

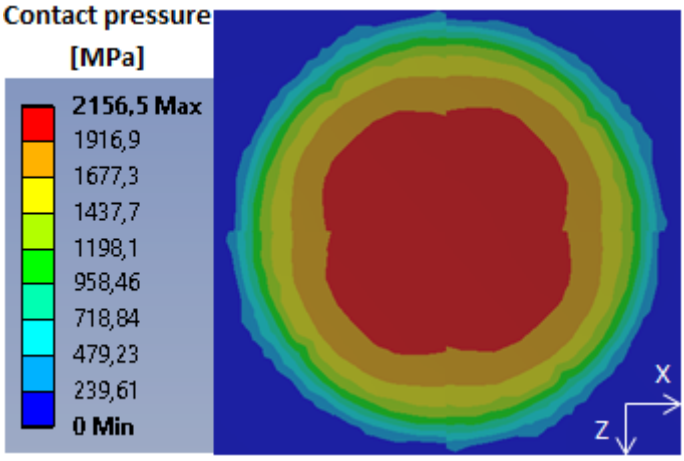

Figure 3 *Contact pressure using a force of 200 N*

Contact pressure is similar for the Hertz and elastic-plastic FE simulation up to the force of 100 N, see Figures 4 and 5. The differences are more pronounced for force 150 N (and higher), where the maximum Equivalent plastic strain overcomes 0.01 [-], as illustrated in Figures 4 and 5. The maximum contact pressure decreases with increased Equivalent plastic strain; compare Figures 4 and 5.

For the given geometry and material, Hertz contact pressure can be used for estimation of a loading up to the force of 100 N.

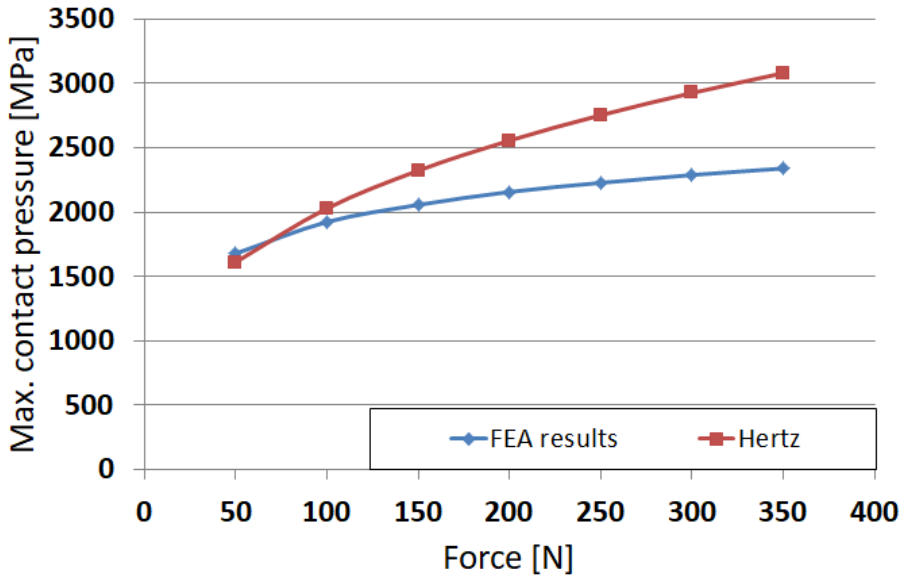

Figure 4 *Comparison of the computed maximum contact pressure (FEA results) with Hertz (linear-elastic) contact pressure*

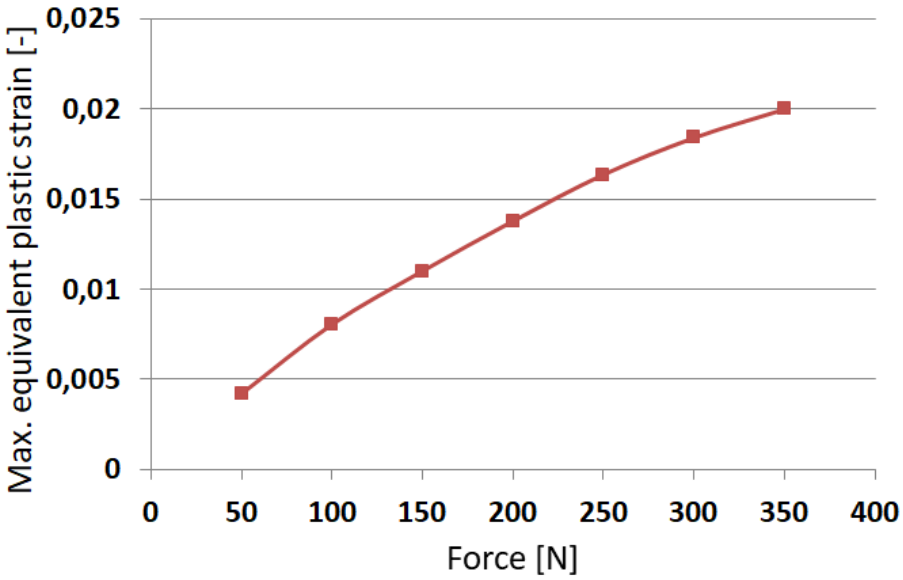

Figure 5 *Maximum of the equivalent plastic strain (material 1.4545)*

Figure 6 shows the remaining indentation depth after the unloading in the centre of the contact patch on the planar surface (see also Figure 3). The indentation depth is in order of a surface roughness, and no implications in terms of notch effect are assumed.

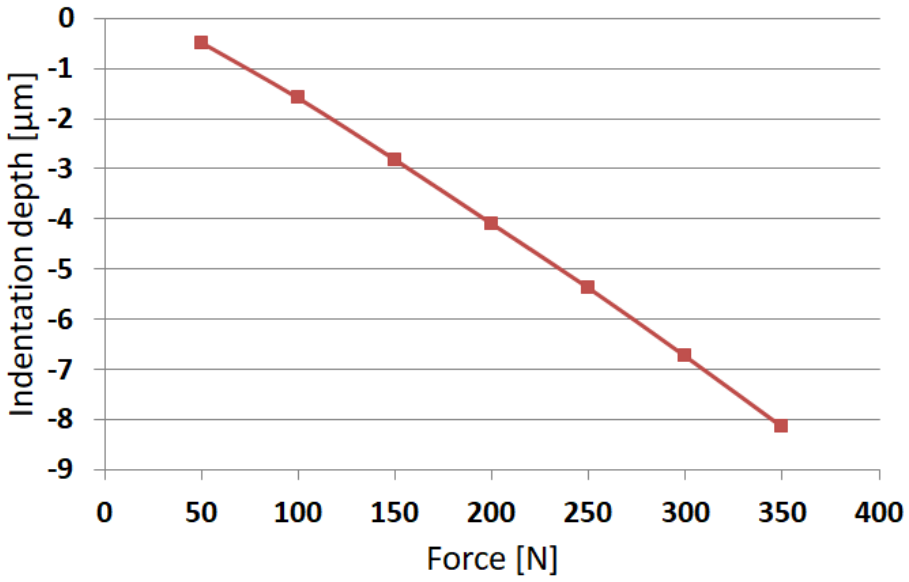

Figure 6 *Remaining indentation depth on the planar surface after the unloading in the centre of the contact patch*

DISCUSSION ON RESULTS

The presented FE model does not take into account cyclic loading (cyclic plasticity), residual stresses and surface roughness; generally speaking, technological inheritance. Such influences are supposed to be sufficiently covered in the coefficients in the design guides, as presented for instance in [18].

The methodology of designing the machine parts subjected to elastic-plastic conditions can be divided into the following points:

1. Designing a bilinear (or other) material model.
2. Performing the static elastic-plastic FE contact simulation with obtained true stress-strain data for the given geometry.
3. Comparing the contact stresses with the Hertz contact pressure (elastic FE simulation).
4. Taking into account the type of loading (dynamic, stochastic etc.) and technological inheritance by choosing coefficients from the design guide.

CONCLUSIONS

The elastic-plastic FE contact simulation was performed to estimate a contact loading of a machine part. The plastic response of the material 1.4545 was studied using a bilinear material model. As the results, a methodology of designing the machine parts subjected to elastic-plastic contact conditions was proposed. The methodology combines a measured (or datasheet) material data, FE simulation and coefficients from design guides.

References

[1] NEMETZ, A. W. et al. 2018. FE temperature- and residual stress prediction in milling inserts and correlation with experimentally observed damage mechanisms. *Journal of Materials Processing Technology*, **256**, pp. 98-108. [Online]. http://www.sciencedirect.com/science/article/pii/S0924013618300402

[2] BRECHER, CH., ESSER, B., FALKER, J., KNEER, F., FEY, M. 2018. Modelling of ball screw drives rolling element contact characteristics. *CIRP Annals*, **67**, pp. 409-412, 2018. [Online]. http://www.sciencedirect.com/science/article/pii/S0007850618301331
[3] MAO, K. 2007. Gear tooth contact analysis and its application in the reduction of fatigue wear. *Wear*, **262**, pp. 1281-1288. [Online]. http://www.sciencedirect.com/science/article/pii/S0043164806002687
[4] WIEST, M., KASSA, E., DAVES, W., NIELSEN, J. C. O., OSSBERGER, H. 2008. Assessment of methods for calculating contact pressure in wheel-rail/switch contact. *Wear*, 265, pp. 1439-1445, Contact Mechanics and Wear of Rail/Wheel Systems - CM2006. [Online]. http://www.sciencedirect.com/science/article/pii/S0043164808001798
[5] MAJZOOBI, G. H., ABBASI, F. 2017. On the effect of shot-peening on fretting fatigue of Al7075-T6 under cyclic normal contact loading. *Surface and Coatings Technology*, **328**, pp. 292-303. [Online]. http://www.sciencedirect.com/science/article/pii/S0257897217308770
[6] KRÁČALÍK, M., TRUMMER, G., DAVES, W. 2016. Application of 2D finite element analysis to compare cracking behaviour in twin-disc tests and full scale wheel/rail experiments. *Wear*, **346-347**, pp. 140-147. [Online]. http://www.sciencedirect.com/science/article/pii/S0043164815004895
[7] WEI DA-SHENG, SHI LIANG, WANG YAN-RONG. 2015. Cyclic plastic behavior of dovetail under fretting load. *Engineering Failure Analysis*, **55**, pp. 100-114. [Online]. http://www.sciencedirect.com/science/article/pii/S1350630715001594
[8] SASAGAWA, K., NARITA, J. 2017. Development of thin and flexible contact pressure sensing system for high spatial resolution measurements. *Sensors and Actuators A: Physical*, **263**, pp. 610-613. [Online]. http://www.sciencedirect.com/science/article/pii/S0924424716305635
[9] DU FEI, LI BAOTONG, ZHANG JIE, QUAN ZHU MIN, HONG JUN. 2015. Ultrasonic measurement of contact stiffness and pressure distribution on spindle–holder taper interfaces. *International Journal of Machine Tools and Manufacture*, **97**, pp. 18-28. [Online]. http://www.sciencedirect.com/science/article/pii/S0890695515300523
[10] DÖRNER, F., KÖRBLEIN CH., SCHINDLER, CH. 2014. On the accuracy of the pressure measurement film in Hertzian contact situations similar to wheel-rail contact applications. *Wear*, vol. 317, pp. 241-245. [Online]. http://www.sciencedirect.com/science/article/pii/S0043164814001975
[11] SOLLE, J., LINARES, J. M., SPRAUEL, J. M., MERMOZ, E. 2012. Optical measurement for the estimation of contact pressure and stress. *CIRP Annals*, **61**, pp. 483-486. [Online]. http://www.sciencedirect.com/science/article/pii/S0007850612001308
[12] HAN XINGHUI, HUA LIN. 2013. 3D FE modelling of contact pressure response in cold rotary forging. *Tribology International*, **57**, pp. 115-123. [Online]. http://www.sciencedirect.com/science/article/pii/S0301679X12002502
[13] NAJJARI, M., GUILBAULT, R. 2014. Modeling the edge contact effect of finite contact lines on subsurface stresses. *Tribology International*, **77**, pp. 78-85. [Online]. http://www.sciencedirect.com/science/article/pii/S0301679X1400156X
[14] BLANCO-LORENZO, J., SANTAMARIA, J., VADILLO, E. G., CORREA, N. 2018. A contact mechanics study of 3D frictional conformal contact. *Tribology International*, **119**, pp. 143-156. [Online]. http://www.sciencedirect.com/science/article/pii/S0301679X17304863
[15] Datasheet: 1.4545 (15-5PH®), S155500 | METALCOR
[16] FARAHMAND, B., NIKBIN, K. 2008. Predicting fracture and fatigue crack growth properties using tensile properties, *Engineering Fracture Mechanics*, **75**, pp. 2144-2155. [Online]. http://www.sciencedirect.com/science/article/pii/S0013794407003888
[17] JOHNSON, K. 1985. *Contact Mechanics*. Cambridge: Cambridge University Press. doi:10.1017/CBO9781139171731
[18] FKM2012; Rechnerischer Festigkeitnachweis für Maschinenbauteile. 2012: VDMA Verlag, ISBN 978-3-8163-0605-4 (in German)

ORCID

Michal Kráčalík 0000-0002-7938-403X